CCC 2008 - Challenges for Civil Construction
Torres Marques et al. (Eds)

EXPLORING THE POSSIBILITIES OF A NEW TECHNIQUE FOR THE SHEAR STRENGTHENING OF RC ELEMENTS

Joaquim A. O. Barros[*], Gláucia M. Dalfré[*], Elisa Trombini[†] and Alessandra Aprile[†]

[*] ISISE, DEC, School of Engineering, University of Minho
Campus de Azurem, 4800-058 Guimarães, Portugal
e-mail: barros@civil.uminho.pt, gmdalfre@civil.uminho.pt, web page: http://www.civil.uminho.pt/composites

[†] Dep. Civil. Eng., University of Ferrara
Via Saragat, 1 - 44100 Ferrara, Italy
e-mail: elisa.trombini@hotmail.it, prllsn@unife.it

Keywords: CFRP round bars, Shear strengthening, Reinforced concrete elements, CDM technique.

Summary: *In the present work, the possibilities of a CFRP-based strengthening technique, herein designated Core Drilled Mounted (CDM) technique, to increase the shear resistance of reinforced concrete (RC) elements were explored. For this purpose, an exploratory experimental program of short beam shear specimens was carefully carried out with the purpose of capturing the main features of the CFRP bar contribution for the concrete shear resistance. The adopted monitoring system was able of establishing a relationship between crack opening, crack sliding and strains in the CFRP strengthening bar, for each applied load. From the obtained results it was observed that a CFRP reinforcement ratio of 0.2% contributed for a 26% increment in terms of specimen shear resistance. Furthermore, at a crack width of 0.3 mm the strain level in the CFRP was enough significant to show that this is a promising strengthening technique for the shear and punching resistance of RC structures. It was also observed that the contribution of the CFRP bars was more effective when concrete cohesive failure mode occurred, indicating that bar-adhesive debond failure mode should be avoided, which requires to select the most appropriate FRP-adhesive system.*

1 INTRODUCTION AND THE STRENGTHENING CONCEPT

Near-Surface Mounted (NSM) is one of the latest and most promising strengthening techniques for the increase of the flexural [1,2] and shear resistance [3-7] of reinforced concrete (RC) beams. Due to its easy application, NSM is particularly suitable to increase the negative bending moments of continuous RC structures [8]. However, the NSM efficacy can be compromised by the shear resistance of the RC element [9], due to the possibility of forming shear failure cracks (see Figure 1). To avoid the occurrence of this brittle failure mode, NSM can also be used in case of beams, applying CFRP strips into grooves opened on the concrete cover of the beam's lateral faces [3-7]. In case of slabs, the NSM shear strengthening has no sense, and the technique herein designated as Core Drilled Mounted (CDM) can be a competitive strengthening strategy to increase the shear resistance of RC slabs. The CDM strengthening concept is schematically represented in Figure 1. The CDM can also be used to increase the punching resistance of RC slabs, as well as the shear resistance of RC beams. According to the CDM technique, holes are opened across the slab/beam thickness, with the desired inclinations, and FRP circular cross section bars are introduced into these holes and bonded to the concrete substrate with adhesive materials. A step forward in the effectiveness of this technique can be done applying the FRP bars with a certain pos-tension, a topic that will be explored in a next future. This is especially opportune in shear cracked beams, since the pos-tension can close these already existing cracks, which increases the concrete aggregate interlock effect. Furthermore, in pre-cracked shear elements, the direction of the FRP bars can be selected in order to provide the most effective shear strengthening.

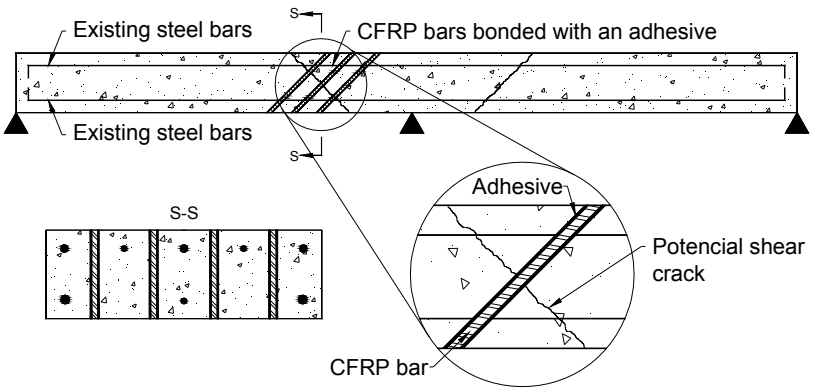

Figure 1: CDM strengthening technique for slab/beam RC elements

2 SPECIMEN, STRENGTHENING TECHNIQUE, TEST SETUP AND MATERIAL PROPERTIES

2.1 Specimen

Before starting a large experimental program in the CDM domain, it is recommendable the execution of preliminary tests to explore the possibilities of the concept, extract relevant information about the test setup, and define a monitoring system able to capture essential data. These tests should also provide results that can highlight crucial indicators about the CDM shear strengthening effectiveness. For this purpose, the short beam shear specimen [10] and the test setup represented in Figure 2 were assumed as having the possibility of simulating the CDM shear strengthening phenomena in a RC slab. The test program was composed of two equal specimens, subjected to a monotonic loading configuration that can reproduce, as nearest as possible, the stress field on a shear failure zone of shear deficiently RC elements. The notation adopted to identify each specimen is CSx, where “x” is the specimen number.

2.2 Measuring Devices

A servo-controlled test equipment was used, where the load applied by the servo-actuator of 200 kN load capacity was controlled by the signal imposed to its LVDT, at a displacement rate of 2μm/s, in order to assure stable tests. The force was measured by a load cell of 200 kN maximum capacity and 0.5% linearity. To evaluate the crack opening of the shear failure crack, three LVDTs of ±0.5 mm and ±2.5 mm full stroke were used in the first and the second test, respectively, whereas one LVDT of ±5 mm was used to record the sliding of the shear failure crack. The arrangement of displacement transducers and the position of the strain gauges at the CFRP bar are represented in figure 3. The SG1 coincides with the shear crack plane.

2.3 Strengthening technique

Concrete specimens were strengthened at approximately 15 days of age. The notches, necessary to induce crack propagation (a fracture sliding-opening mixed mode), were made by a diamond saw cut machine and had about 5 mm width and 10 mm depth on the concrete cover of the specimens, in the alignment with the loading plane.

A hole of 12 mm diameter was made across the specimen using an electric machine. The hole was cleaned with compressed air before bonding the CRFP bar to the concrete. The CFRP bar was cleaned with acetone to remove any possible dirt. The adhesive was prepared according to the supplier recommendations and the CRFP bar was introduced into the hole, which was filled with resin, resulting an adhesive layer of about 2 mm thickness. At least five days were spent on the curing/hardening process of the epoxy adhesive, before testing the specimen. Figure 4 shows some phases of the CDM strengthening technique.

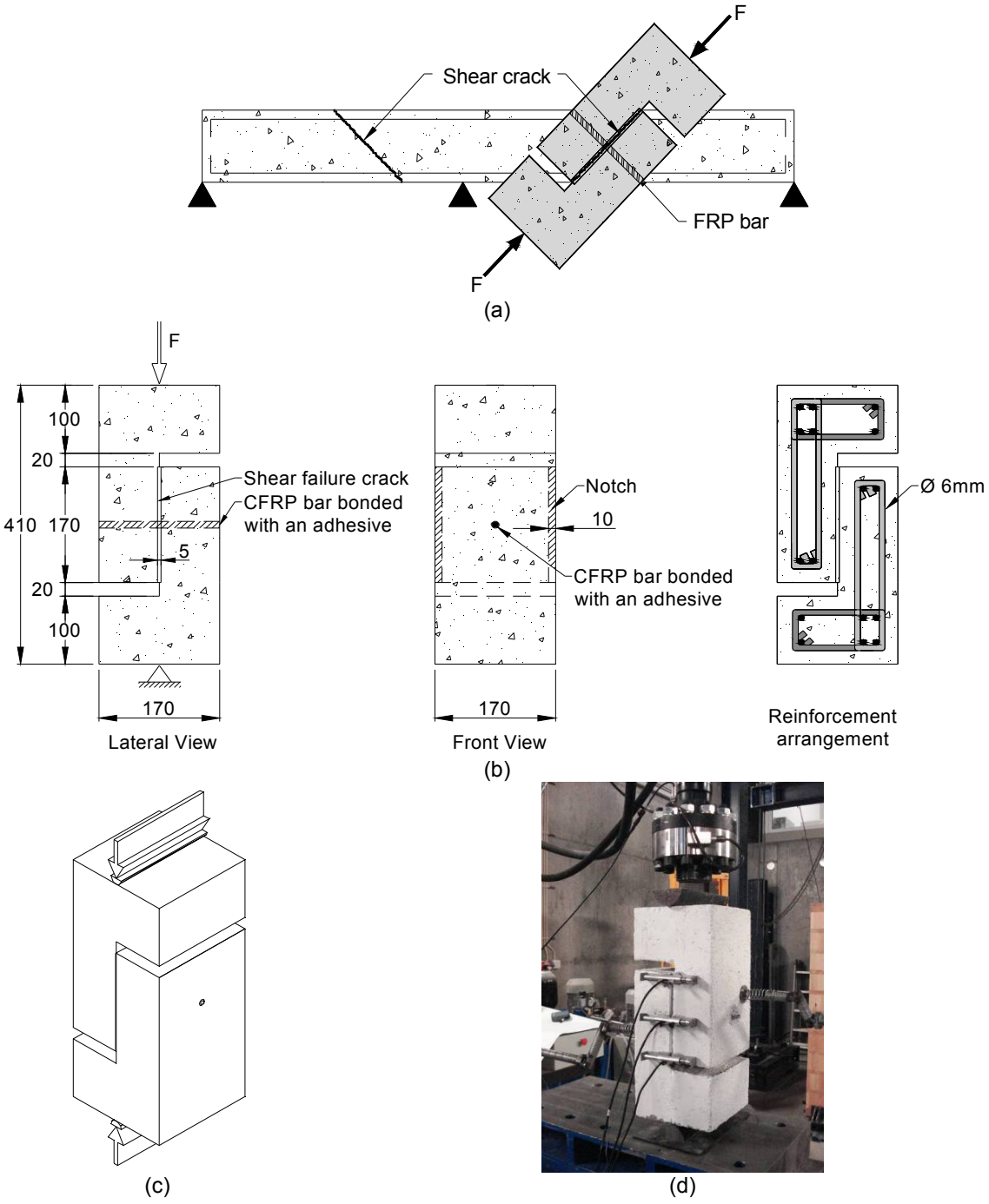

Figure 2: (a) Concept, (b) specimen cross-section dimensions (in mm); (c) 3D perspective of the specimen; (d) photo of the test setup

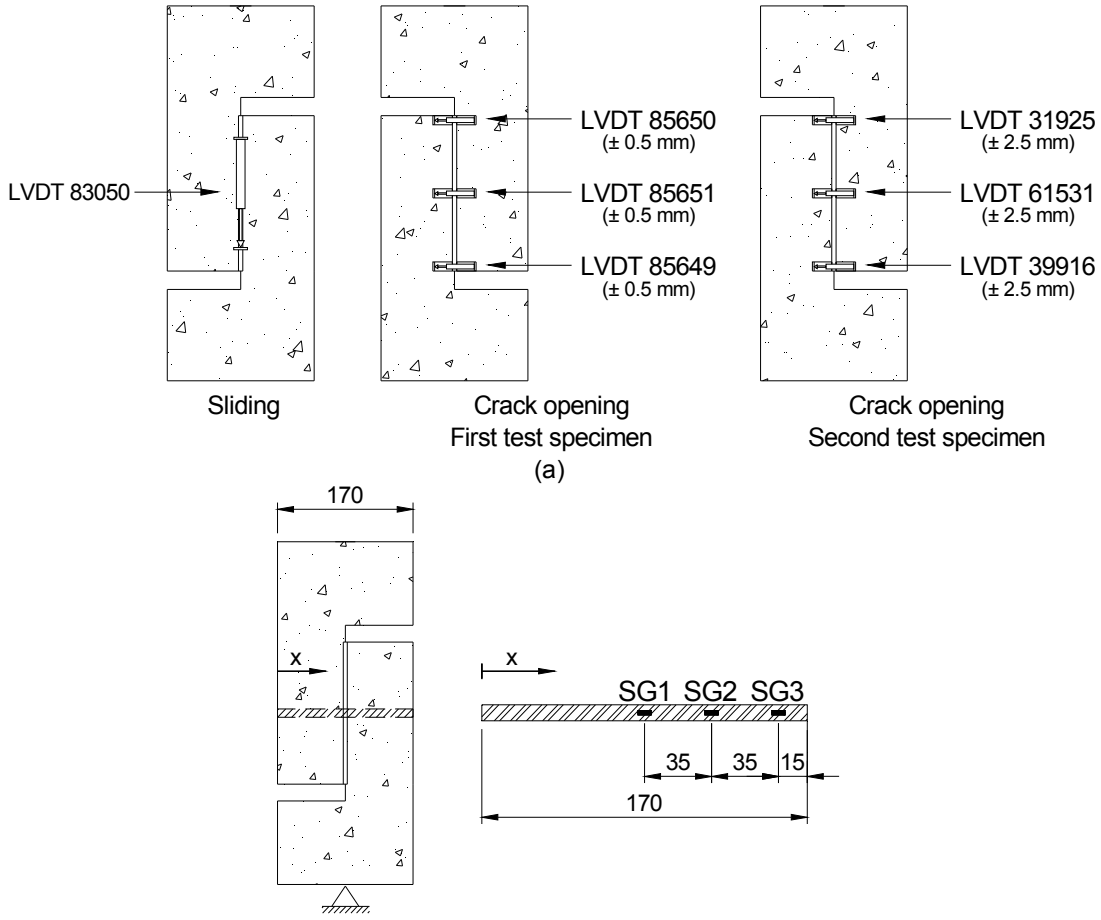

Figure 3: (a) Arrangement of the LVDTs and (b) lay-out of the strain gauges (SG) at the CFRP bar

2.4 Materials properties

2.4.1 Concrete

The concrete compressive strength was determined from uniaxial compression tests carried out on cubes of 150 mm edge, at the age of about 20 days, when the specimens were tested. The concrete average compressive strength (f_{cm}) was 33.2 MPa, with a standard deviation of 2.6 MPa.

2.4.2 CFRP bars

CFRP bars with sand coated surface were used in the present experimental program. Twenty measurements were executed, having been obtained a diameter of 8.31 ± 0.14 mm. To evaluate the tensile strength of the CFRP bars, uniaxial tensile tests were carried out in a servo controlled test machine, according to the recommendations of ISO 527-5 [11]. From these tests, a tensile strength of 1145 MPa was obtained. Another program of tensile tests are being carried out to evaluate the Young's Modulus of the CFRP bars, and the results will be presented in a next publication.

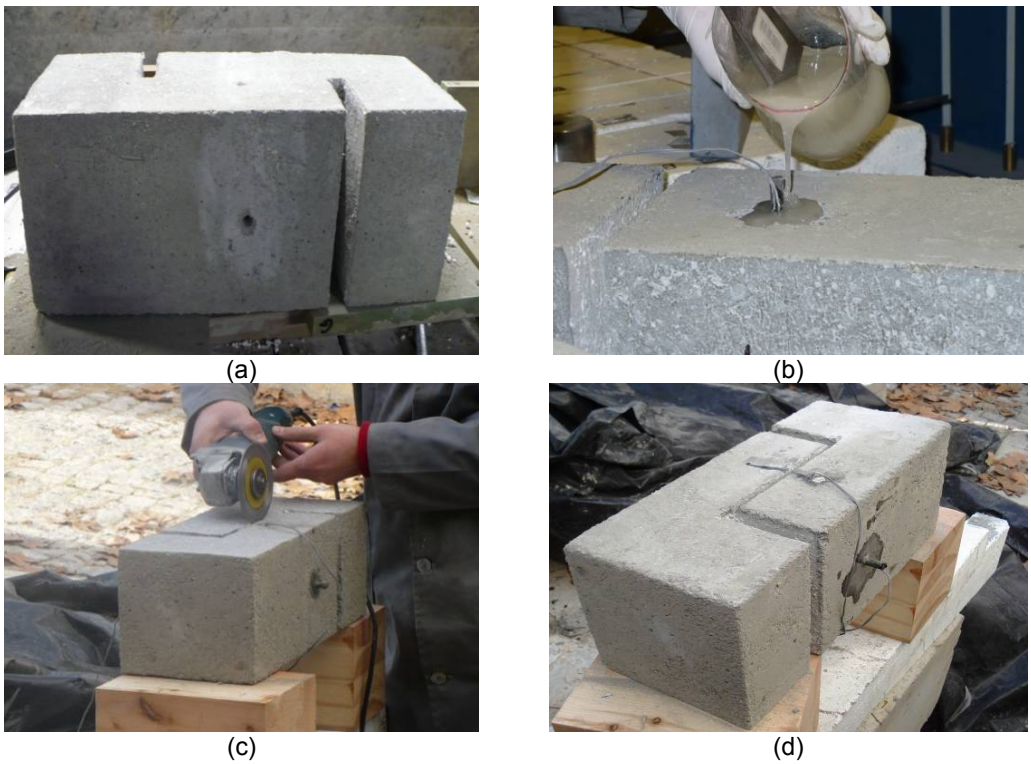

(a) (b) (c) (d)

Figure 4: Phases of the CDM strengthening technique

2.4.3 Adhesive

An epoxy resin-based bond agent with a trademark of S&P - Resin 55 was selected to bond the CFRP bars to concrete. From the uniaxial tensile tests, with the specimens represented in Figure 5a, carried out according to the recommendations of ISO 527-5 [11], the stress-strain curves depicted in Figure 5b were obtained. A high homogeneity in terms of stress-strain response was registered, and all the tested specimens failed near its center cross section (see Figure 5c). The strains were measured with a clip and strain gauge, for assessing the possibility of using the former one in the future programs for the characterization of adhesive materials. From the tensile tests, a Young´s modulus of 2.19 GPa and a tensile strength of 36.2 MPa were obtained.

3 PRESENTATION AND DISCUSSION OF THE RESULTS

3.1 Crack patterns and failure modes

Before attaining the maximum applied load, the horizontal, followed by the vertical cracks, shown in Figure 6a, formed due to tensile stress gradients derived from local bending moments at the cross sections of relative smaller flexural stiffness. However, since the specimens failed at the notched plane, the formation of these cracks had no influence on the main objectives of the present study. Before the maximum load has been attained, it was visible the formation of a crack in the notched plane (Figure 6b).

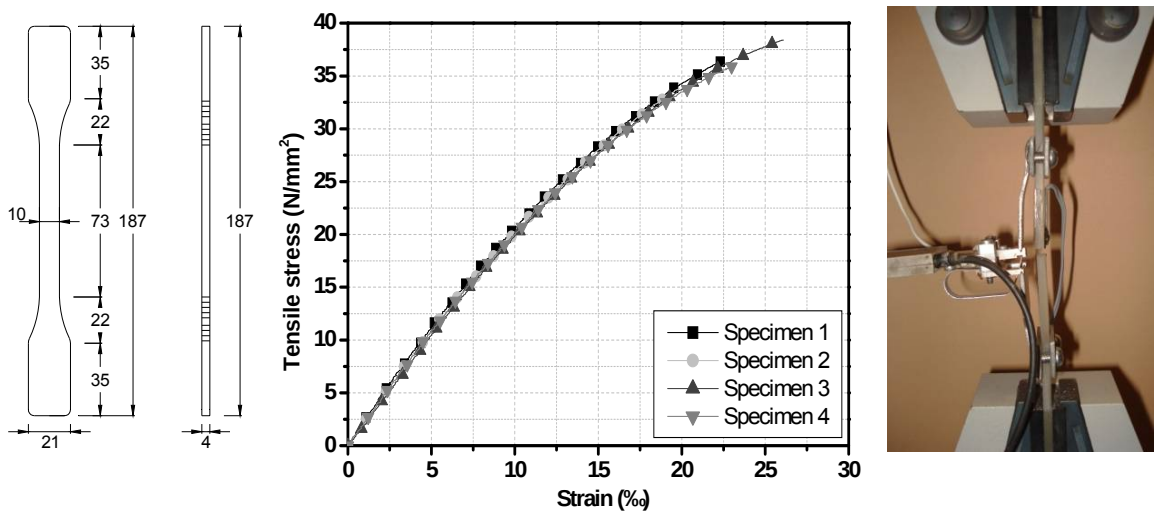

Figure 5: (a) Adhesive specimen dimensions (in mm), (b) stress-strain curves, and (c) failure mode

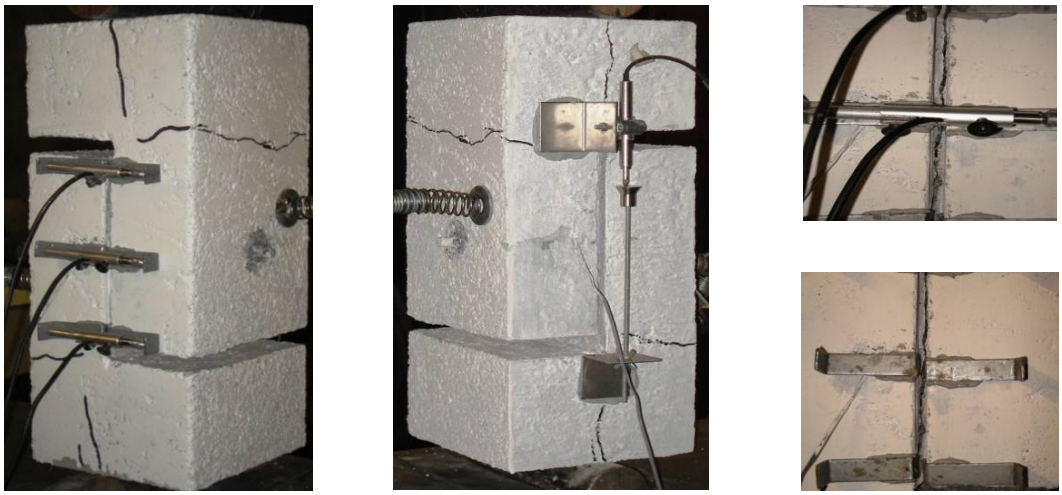

Figure 6: Cracks (a) outside and (b) in the notched shear failure plane

The sliding and the opening of this crack increased up to peak load but, due to the resistance to crack opening offered by the CFRP bar, as well as due to its relative reduced shear stiffness, the sliding increase was more pronounced than the crack opening increase (see, for a while, Figure 8). The CFRP bar also contributed to increase the effect of the concrete aggregate interlock for the shear resistance, since its elastic axial stiffness and debond resistance introduced a stress field normal to the shear crack, resulting a Mohr-Coulomb like-beneficial effect.

After having been tested, it was observed that, in the CS1 specimen a debond occurred at bar-adhesive interface, while in the CS2 specimen a concrete layer of irregular profile was attached to the epoxy adhesive along the debond length of the CFRP bar (see Figure 7).

(a) (b)

Figure 7: Failure modes: (a) CS1 and (b) CS2 specimens

3.2 Force-crack opening and sliding responses

Figure 8 shows the relationship between the applied force and both the crack opening (at the LVDT placed at the level of the CFRP bar – intermediate LVDT, see Figure 3a) and crack sliding.

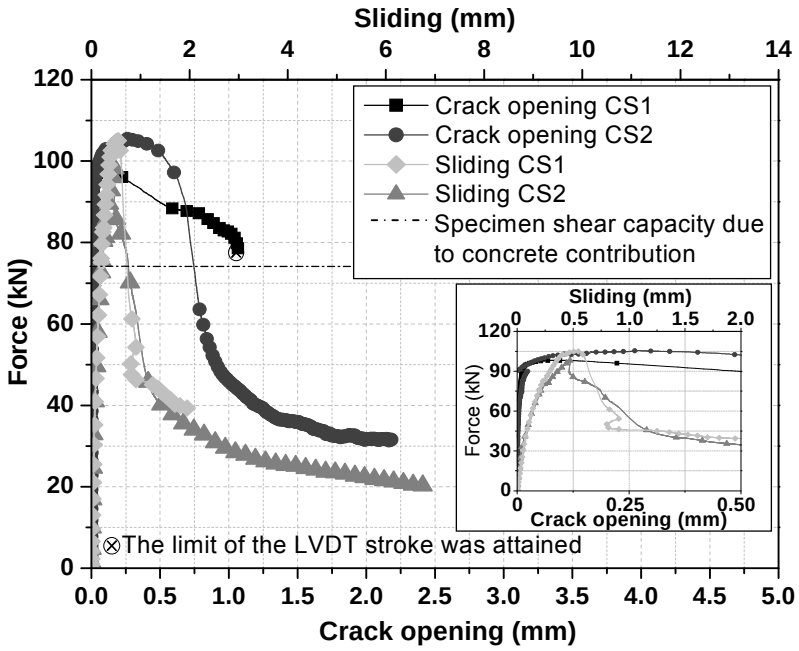

Figure 8: Force-sliding-crack opening curves

In this figure it is also represented the concrete contribution for the shear resistance (horizontal line). Taking the average concrete compressive strength obtained in the experimental tests, and using the recommendations of the EC2 [12], it was obtained a concrete shear strength of τ_c= 0.15 fck = 2.9 MPa (fck is the characteristic value of the cylinder concrete compressive strength), which results in an average concrete shear force of 2.9×150×170/1000.0=74.9 kN. Since the average peak load registered in the two tested specimens was 101.7 kN, it can be concluded that a CFRP bar of 54 mm^2 cross section

area, per a shear failure crack area of 25500 mm^2 (a CFRP reinforcement ratio of 0.2%), had a contribution of 26% for the specimen shear resistance.

Figure 8 shows that sliding was more pronounced than crack opening. However, since the supports of the LVDT that measured the sliding were placed in the zones of the specimen subjected to the highest compression stress field, part of this sliding might be caused by the concrete elasto-plastic deformation of these zones. In the experimental program that is now in preparation, the supports of this LVDT will be installed at the faces of the notch, in order to minimize this effect. The inset of Figure 8 shows that, from a crack width between 0.02 mm and 0.5 mm the specimen load carrying capacity was almost maintained, in spite of having occurred a phase of sliding hardening and sliding softening during this loading period of the specimens. It is quite impressive the similar behavior of both specimens up to a crack opening of 0.5 mm, which, for the majority of model codes dedicated to the design of concrete structures, is the maximum admissible crack width. The pullout resisting force of the CFRP bar contributed to the specimen pseudo-plastic behavior registered in this phase. The loaded end slip of the CFRP bar pullout, at the shear crack plane, degenerates in the opening of the shear failure crack. For loaded end slip values up to about 0.25 mm (it is reasonable to assume that crack opening is about two times the CFRP loaded end slip) the force to pullout out the CFRP bar was high enough to almost sustain the maximum load applied to the specimens.

Table 1 resumes relevant obtained results. At maximum force the maximum sliding, crack opening and CFRP strain did not exceed 0.55 mm, 0.3 mm and 2.74‰, respectively. With the propagation of the crack opening and crack sliding, the strain in the CFRP bar increased, having attained maximum values of 5,10 and 7,74‰.

Table 1 : Relevant results

Specimen	Maximum force [kN]	Crack sliding [mm]	Crack opening [mm]	SG1 strain at maximum force [‰]	Ultimate SG1 strain [‰]
CS1	98.27	0.47	0.1	0.38	5.10
CS2	105.04	0.55	0.3	2.74	7.74

Figure 9 shows three distinct phases in terms of crack opening versus crack sliding. In the first branch, a significant increase of sliding occured with a marginal crack opening.

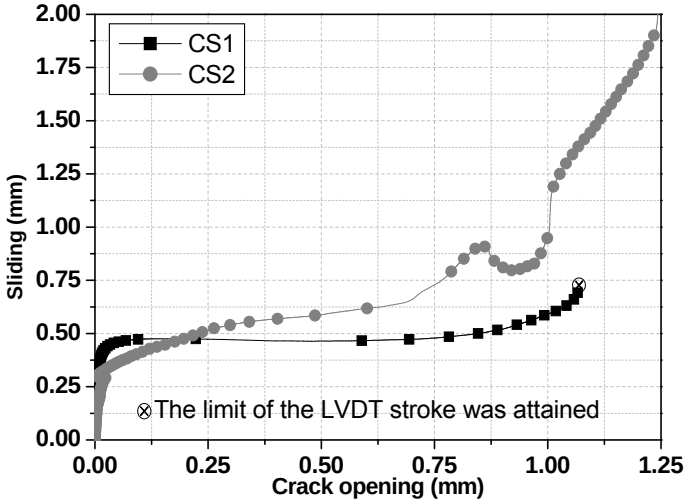

Figure 9: Sliding-crack opening curves

This phase ended at a level in the range of 80 to 90% of the peak load, in its hardening branch. As already mentioned, significant part of this sliding might be justified by the concrete compressive deformation captured by the LVDT that was installed to measure the crack sliding. Therefore, the displacement measured by this LVDT might not represent the real relative slid movement of the two faces of the shear failure crack. In the second phase, for a reduced increment of sliding a pronounced increase of crack opening occurred. This means that, to overcome the asperities (aggregate interlock) of the shear failure crack, the width of the crack needed to increase considerably. After the resistance to the crack sliding, offered by the mechanical interlock of the aggregates, has been exhausted, which happened for a crack width of about 1.0 mm, a new phase occurred, being characterized by an increase of both crack width and crack sliding, but this last one was more pronounced. In CS1, due to the attainment of the limit of the stroke of the LVDT used to measure the crack width, the maximum registered crack width corresponds to this limit.

Figure 10 depicts the relationship between the applied force and the strains recorded in the SG1 strain gauge installed on the CFRP bars. In CS1 specimen an almost linear relationship between applied load and SG1 strain was obtained up to peak load. At peak load the strain was 0.38‰ (see Table 1), but after the formation of the shear failure macro-crack, a significant increment of the SG1 occurred followed by a smooth decrease of the applied load, up to a strain level of about 4‰. In this smooth structural softening phase, the contribution of the CFRP bar-adhesive bond resistance was decisive to maintain the shear residual capacity in a high level. After this phase, a pronounced decrease of the specimen load carrying capacity occurred, followed by a small increase of the SG1 strain, up to the collapse of the specimen, which happened for a strain of about 5.1‰.

In case of CS2 specimen, since an irregular thickness of concrete layer was attached to the epoxy adhesive of the part of the CFRP bar that debonded, a more cohesive failure mode occurred in this specimen, when compared to what happened in the CS1 specimen. This distinct failure mode of the CFRP bar contributed to mobilize more effectively the CFRP bar, having resulted a strain hardening branch before peak load, higher specimen load carrying capacity, and higher strain values on the bar of the CS2 specimen.

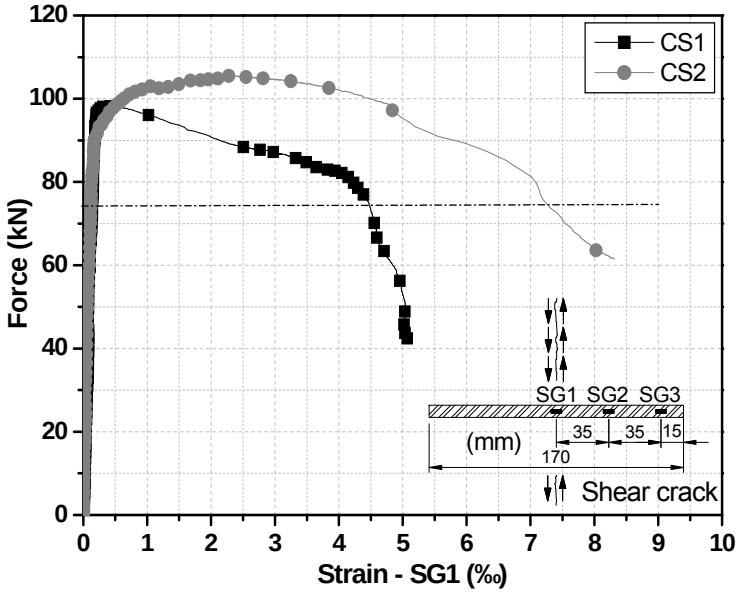

Figure 10: Relationship between the applied force and the SG1 strains in the CFRP bar

Since crack opening limit is a mandatory condition in the design and strengthening of RC structures, the relationship between the crack opening and the SG1 strains is depicted in Figure 11 (SG1 is at the shear failure crack plane). Due to the distinct failures modes of the CFRP bar of the two tested specimens, the contribution of the CFRP bar of CS2 specimen was more effective, regardless the level of crack opening. For the maximum crack opening values recommended by the RC design model codes, the SG1 strain values installed in the CFRP bars are those included in Table 2. For the crack widths of 0.3 and 0.5 mm the strains are relatively significant, but they can be increased if a smaller adhesive layer thickness is used, or an adhesive of higher elasticity modulus is selected.

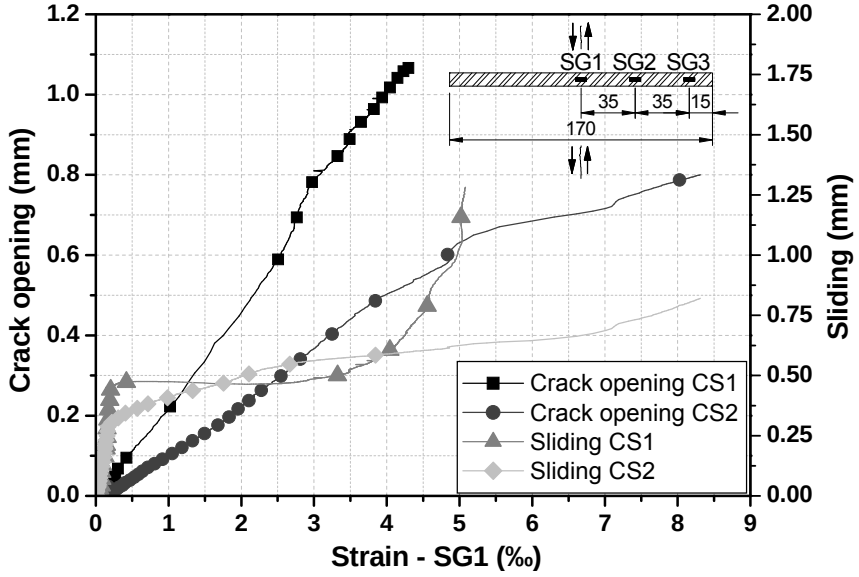

Figure 11: Relationship between the crack opening, crack sliding and the SG1 strains in the CFRP bar

Table 2: Strain values at the SG1 for distinct levels of crack opening

Crack opening (mm)	Strain SG1 (‰)	
	CS1	CS2
0.1	0.44	1.00
0.3	1.36	2.56
0.5	2.17	3.99

4 CONCLUSIONS

In the present work, the possibilities of a CFRP-based strengthening technique to increase the shear resistance of reinforced concrete (RC) elements were explored. For this purpose, an exploratory experimental program of short beam shear specimens was carefully carried out with the purpose of capturing the main features of the CFRP bar contribution for the concrete shear resistance. The adopted monitoring system was able of establishing a relationship between crack opening, crack sliding and strains in the CFRP strengthening bar, for each applied load. From the obtained results it was observed that a CFRP reinforcement ratio of 0.2% contributed for a 26% increment in terms of specimen shear resistance. Furthermore, at a crack width of 0.3 mm the strain level in the CFRP was enough significant to show that this is a promising strengthening technique for the shear and punching resistance of RC structures. It was verified that the contribution of the CFRP bars was more effective

when concrete cohesive failure mode occurred, indicating that bar-adhesive debond failure mode should be avoided, requires to select the most appropriate FRP-adhesive system. A large experimental program is now being prepared to assess the influence of the following parameters on the contribution of FRP bars for the shear resistance of RC beams and slabs: concrete strength class; relative orientation between FRP bars and crack shear failure plane; adhesive properties; bond length; material and surface characteristics of the FRP bars.

5 ACKNOWLEDGEMENTS

The authors wish to acknowledge the support provided by the "Empreiteiros Casais", S&P®, Secil (Unibetão, Braga) Companies. The study reported in this paper forms a part of the research program "CUTINEMO - Carbon fiber laminates applied according to the near surface mounted technique to increase the flexural resistance to negative moments of continuous reinforced concrete structures" supported by FCT, PTDC/ECM/73099/2006. The second author would like to acknowledge the National Council for Scientific and Technological Development (CNPq) – Brazil for financial support for scholarship (GDE/CNPq).

REFERENCES

[1] J.A.O. Barros and A.S. Fortes, *Flexural strengthening of concrete beams with CFRP laminates bonded into slits*, Journal Cement and Concrete Composites, 27(4), 471-480, (2005).

[2] R. El-Hacha, S.H. Rizkalla, *Near-surface-mounted fiber-reinforced polymer reinforcements for flexural strengthening of concrete structures*, ACI Structural Journal, 101(5), 717-726, (2004).

[3] A. Carolin, *Carbon fibre reinforced polymers for strengthening of structural elements*, PhD thesis, Lulea University of Technology (2003).

[4] J.A.O. Barros and S.J.E. Dias, *Near surface mounted CFRP laminates for shear strengthening of concrete beams*, Journal Cement and Concrete Composites, Vol. 28, N. 3, pp. 276-292 (2006).

[5] S.J.E. Dias and J.A.O. Barros, *NSM CFRP Laminates for the Shear Strengthening of T Section RC Beams*, 2nd International fib Congress, Naples, Italy, Paper ID 10-58 in CD (2006).

[6] L. de Lorenzis and A. Rizzo, *Behaviour and capacity of RC beams strengthened in shear with NSM FRP reinforcement*", 2nd International fib Congress, Naples, Italy, Paper ID 10-9 in CD (2006).

[7] S.J.E. Dias, V. Bianco, J.A.O. Barros, G. Monti, *Low strength concrete T cross section RC beams strengthened in shear by NSM technique*, Workshop-Materiali ed Approcci Innovativi per il progetto in zona sismica e la mitigazione della vulnerabilità delle strutture, University of Salerno, Italy, 12-13 February (2006).

[8] E. Bonaldo, *NSM technique for the flexural strengthening of RC slab structures (Provisory Title)*, PhD Thesis, University of Minho, In Preparation.

[9] E. Bonaldo, J.A.O. Barros, P.J.B. Lourenço, *Influence of the spacing between NSM-CFRP laminates on the flexural strengthening efficacy of RC slabs*, FRPRCS-8, University of Patras, Patras, Greece, July 16-18, (2007).

[10] B.I.G. Barr, E.B.D. Hasso, K. Liu, *Shear strength of FRC materials*, Composites, 16(4), 326-334, (1985).

[11] ISO 527-5. Plastics - Determination of tensile properties - Part 1: Test conditions for unidirectional fibre-reinforced plastic composites, International Organization for Standardization, Genèva, Switzerland, 9 pp., (1993).

[12] Eurocode 2: Design of concrete structures - part 1: General rules and rules for buildings EN 1992-1-1:2004:E. Brussels: European Committee for Standardization, December (2004).